

Meron ground states of quantum Hall dropletsM. V. Milovanović,¹ E. Dobardžić,² and Z. Radović²¹*Institute of Physics, P.O. Box 68, 11080 Belgrade, Serbia*²*Department of Physics, University of Belgrade, P.O. Box 368, 11001 Belgrade, Serbia*

(Received 15 May 2009; revised manuscript received 30 June 2009; published 10 September 2009)

We argue that topological meron excitations, which are in a strong coupling phase (bound in pairs) in infinite quantum Hall ferromagnets, become deconfined in finite-size quantum Hall systems. Although effectively for larger systems meron energy grows with the size of the system, when gyromagnetic ratio is small meron becomes the lowest-lying state of a quantum Hall droplet. This comes as a consequence of the many-body correlations built in the meron construction that minimize the interaction energy. We demonstrate this by using mean-field ansatzes for meron wave function. The ansatzes will enable us to consider much larger system sizes than in the previous work [A. Petković and M. V. Milovanović, *Phys. Rev. Lett.* **98**, 066808 (2007)], where fractionalization into merons was introduced.

DOI: [10.1103/PhysRevB.80.125305](https://doi.org/10.1103/PhysRevB.80.125305)

PACS number(s): 73.43.Cd, 73.21.La

I. INTRODUCTION

A quantum dot (QD) in high magnetic fields,¹ so-called quantum Hall (QH) droplet,² represents an exciting playground for correlation effects in interacting electron systems. Some possible effects can be found in transport measurements that detect oscillations in magnetoconductance³ in the interval $2 \geq \nu \geq 1$ of filling factors. The associated minima of the current amplitude are most completely understood taking into account a tendency of the system to find itself in *depolarized*, highly correlated ground states at some fractions in between despite Zeeman cost.⁴⁻⁷

In this paper we will introduce closely related depolarized states as meron topological excitations of the $\nu=1$ completely polarized droplet, therefore extending topological models to a finite system. They will represent relevant lowest-lying ground-state configurations of the droplet when gyromagnetic ratio is small.

Whenever we think about quasiparticles in small systems we are skeptical about their existence or clear cut description that we can find in infinite systems. That is even more true if we deal with quasiparticles which quantization can be based on topological considerations such as skyrmions in QH ferromagnets.⁸ Nevertheless, as we will argue here, topological objects such as merons, a meron is a half of skyrmion,⁹ can exist as lowest-lying states of a quantum Hall droplet. Therefore fractionalization and quantization, characteristic to QH systems, may persist even in small spin-unpolarized systems bringing topological objects to their description.

The spin characterization of QD states at realistic Zeeman coupling is an open problem.¹⁰ A very thorough understanding of the completely polarized case exists that includes a description of the QD states by the way of a vortex quantization.¹¹⁻¹⁴ The introduction of higher angular momentum states or the increase in magnetic field with respect to the most compact, maximum density configuration of a dot is followed by vortex appearance inside the dot. On the other hand there is a need to introduce a classification to various (partially polarized) states at arbitrary or realistic Zeeman coupling.¹⁵

In the previous work, Ref. 16, by one of the present authors, the Coulomb interaction problem of small quantum

Hall droplets (dots) with $N=4$ and $N=6$, N is the number of electrons, in the limit of zero Zeeman coupling, was studied by exact diagonalization, in the lowest Landau-level approximation. It was shown that the lowest-lying states of these small quantum Hall droplets can be described and classified as states of merons.

In this work we address the question of the existence of meron ground states in large quantum Hall droplets, $N \sim 20$, that exact diagonalizations cannot reach. At the same time, by extrapolation, we will be able to estimate the size of the quantum Hall droplet, $N \sim 100$, at which meron confinement takes place, i.e., when we cannot expect meron ground states. We will be able to do this by using a model wave function that describes a meron of arbitrary winding number positioned at the center of a droplet. In this sense our approach is variational, takes into account a mean-field description of a meron, and compares it energetically first with the ground state—maximum density droplet (MDD) spin-polarized configuration, but also with other meron configurations—of different winding number.

II. DESCRIPTION OF MERON GROUND STATES

At the heart of the theory of the quantum Hall systems at effective small gyromagnetic ratio, and filling factor $\nu=1$, i.e., quantum Hall ferromagnets, is the commensuration of spin and charge deviations from the ground-state values.⁸ Exchange interaction prefers smooth tumbling of spins that follows changes in the charge distribution. Topology plays an important role in the theory of infinite size quantum Hall ferromagnets.⁸ After the spontaneous symmetry breaking the polarization of the ground state is in a definite direction and fixes the boundary condition at infinite radius. Due to then possible mapping between real and internal (spin) spaces, the skyrmion excitations with nontrivial value of topological charge, and the same value of electric charge implied by the commensuration, can be identified. This classical (nonlinear σ model) skyrmion solution finds a concrete quantum-mechanical realization in the following construction⁹

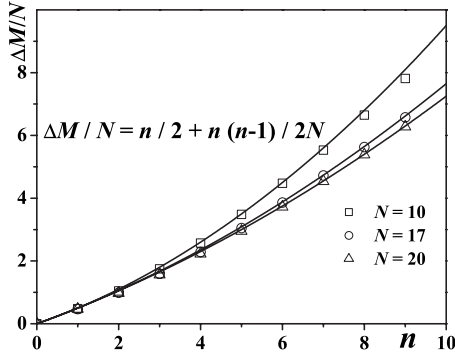


FIG. 1. The mean angular momentum with respect to the ground-state value of the constructions in Eq. (2). The results for various system sizes, i.e., number of electrons (N), are very well fitted with Eq. (3). The fit is better the larger the system size is.

$$\Psi_s = \prod_{i=1}^N \left[\begin{array}{c} \lambda \\ z_i \end{array} \right] \prod_{i<j} (z_i - z_j). \quad (1)$$

We omitted Gaussian factors and z 's are two-dimensional (2D) coordinates of N electrons in the lowest Landau level (LLL) in units of the magnetic length, $l_B = \sqrt{\hbar c/eB}$. In this construction the coordinates (in the orbital part) participate in the spinor part. The complex number λ denotes the size of the skyrmion signifying the characteristic length when the spin, which is around the center pointing up, starts gradually pointing down as it does at infinity ($|z| \rightarrow \infty$). The parameter λ is finite, determined by the ratio between the strength of the interaction and the Zeeman coupling.

Now we specialize to the case of a droplet. We simplify the matters assuming that the gyromagnetic factor is zero. Thus we are in a scale invariant situation where λ may be function only of the size (N) of the system. We take $\lambda \rightarrow c \equiv \sqrt{N}$,¹⁷ and consider constructions for merons of the following form

$$\Psi_m = \prod_{i=1}^N \left[\begin{array}{c} c^n \\ z_i^n \end{array} \right] \prod_{i<j} (z_i - z_j), \quad (2)$$

where n is a positive integer. The mean angular momentum M can be easily (numerically) calculated and with respect to the ground-state value, $M_o = N(N-1)/2$, we find that

$$\Delta M = M - M_o = n \frac{N}{2} + \frac{n(n-1)}{2} \quad (3)$$

approximate very well the calculated ΔM , the better, the larger N is (Fig. 1). Therefore, for $n=1$, the excitation, in the mean, is the excitation of one half of the flux quantum, $\Delta M=N$ being the excitation of (Laughlin's quasi) hole of one flux quantum or a vortex. A skyrmion is a generalization of a Laughlin quasihole in the case of quantum Hall ferromagnets. We may then identify the construction with a classical one for a single meron being "half of the skyrmion," and carrying flux of one half of one flux quantum ($\hbar c/e$). Also its magnetization, from pointing up in the center, gradually transforms into one in the plane ($S_z=0$) on the edges resembling the half of the skyrmion.⁹ In the case of a skyrmion the

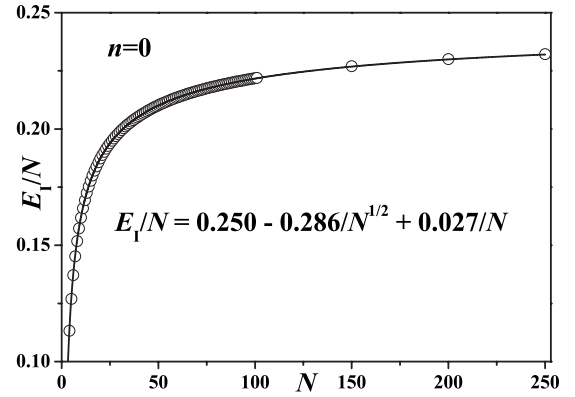


FIG. 2. The ground-state interaction energy per electron in units of V_1 . The analytical fit is an expansion in inverse powers of \sqrt{N} which is the measure of the radius of the system.

magnetization would proceed to transform into configuration that points down on the edges with equal magnitude but opposite direction with respect to the configuration at the center. For a detailed description of the single meron [Eq. (2) with $n=1$] see below and Fig. 5.

Now we will show the results of the calculations of the total (interaction plus confining) energy with respect to a suitable Hamiltonian of the states expressed by Eq. (2). The interaction part of the Hamiltonian we work with can be described as a truncated pseudopotential interaction¹⁸ with only pseudopotentials V_l for $l=0,1$ nonzero and positive. Here l is the relative angular momentum of a pair of electrons in the LLL. Precisely,

$$H_I = \sum_{i<j} \sum_{l=0}^1 V_l P_{ij}^l, \quad (4)$$

where P_{ij}^l is the projector of a state in the LLL of the pair (ij) to the definite relative angular momentum value l . We consider V_0 much larger than V_1 , making the state in Eq. (2) with $n=0$ a unique ground state [up to $SU(2)$ rotation] of the system at filling factor one. In addition to $V_0 \neq 0$ we choose $V_1 \neq 0$ because we want to break energy degeneracy among topological constructions implied by the hard core (only $V_0 \neq 0$) model.¹⁹ For an explanation how to implement the model interaction with pseudopotentials see Appendix. That meron excitations [described in mean field as central constructions by Eq. (2)] are indeed lowest-lying states of a small droplet was shown in Ref. 16 by exact diagonalization in the case of the Coulomb interaction.

The interaction energy of the ground state we calculated taking $V_1=1$ in H_I and the results are plotted in Fig. 2. We see the dependence of the interaction energy per particle on the size—the number of particles in the system. The energy can be very accurately fitted with the analytical expression in the figure as an expansion in inverse powers of \sqrt{N} . (\sqrt{N} is the measure of the radius of the system.) The same analytical expression can be found just considering the sizes up to $N=20$.

The expectation values (interaction energies per particle) of the meron states [Eq. (2) with $n=1,2,3$] with respect to

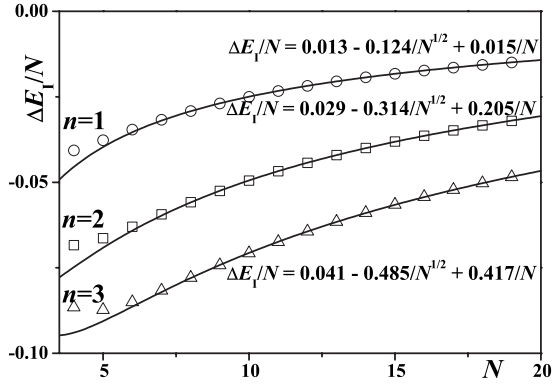


FIG. 3. The interaction energy per electron with respect to the ground-state value for the meron states with $n=1, 2, 3$. Continuous lines depict fits to the calculated values. Fits are expanded in powers of $1/\sqrt{N}$ and the leading term in the $N \rightarrow \infty$ limit is positive. This behavior leads to the absence of merons in large systems.

the ground-state value are plotted in Fig. 3 along with analytical fits. Again we take $V_1=1$ and there are no contributions from the first pseudopotential V_0 because the states in Eq. (2) are zero energy eigenstates with respect to that pseudopotential. The analytical fits are expansions in inverse powers of \sqrt{N} , which is the measure of the radius of the system. The expectation values come with overall negative sign with respect to the ground-state value as each excitation represents an inflation of the volume of the system and therefore increase in the average distance and decrease in the interaction among particles. Nevertheless, we can find extrapolating the fitted analytical expressions to larger number of particles and system sizes that the positive first term (small but always present and approximately proportional to a constant times n) will overcome all other terms in the $N \rightarrow \infty$ limit. This leads to the conclusion that in the thermodynamic limit, $\Delta E_I \sim N$ and positive, the merons are not present in the excitation spectrum. Like vortices in the XY model they are confined in pairs as skyrmion excitations.

In a strong magnetic field and realistic situation with a harmonic confining potential, we can model the confining part of Hamiltonian as

$$H_C = g\Delta M. \quad (5)$$

ΔM is the angular momentum measured with respect to the ground-state value, Eq. (3), and g is a positive constant. Then we may expect [due to the positive third terms in the expressions in Fig. 3 with nearly $n(n-1)$ behavior] that in the case of Hamiltonian,

$$H = H_I + H_C \quad (6)$$

the system is prone to the instabilities (spin reconstructions) described by the meron excitations in Eq. (2). Thus we plotted the total energy of a droplet with $N=19$, Fig. 4, for a few g_c (c critical) when the total energy of the excitation with fixed n equals the energy of the one with $n+1$. This is a situation when one ground state with fixed n becomes less favorable with decreasing g and substituted with another one with the meron number equal to $n+1$. Somehow, as an only

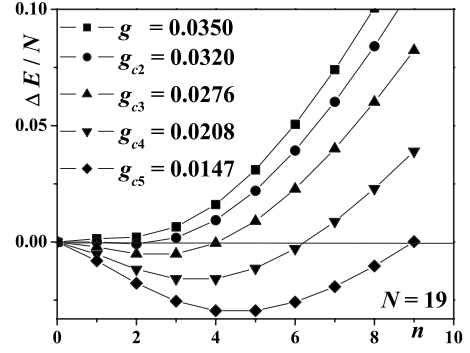


FIG. 4. The total-energy gain per electron as a function of n for $N=19$ and for different values of the confining constant g . There is no meron ground state for $g > 0.032$. Here, g_{ci} , $i=2, 3, 4, 5$ (c for critical) are calculated values of the slope of the confining potential when the total energies for creation of merons with winding numbers $n=i-1$ and $n=i$ are equal. Therefore g_{ci} has the meaning of the slope of the confining potential when meron with higher winding number i enters the droplet.

exception, our mean-field approach predicts that the $n=2$ state reconstruction precedes the one with $n=1$ (Fig. 4). This is very likely an artifact of our choice of the interaction potential [Eq. (4)]. The implied ground states are only possible when the size of the system is not large that the first and the second term in the expansions of the interaction energies become comparable in size. Approximately this happens when $N \gtrsim 100$ as can be seen from the analytical fits in Fig. 3.

With a view on the theory of the evolution of a quantum dot with magnetic field in Ref. 20 in terms of completely polarized states incorporating (quasi)hole excitations, and its reasonable agreement with experiment,²¹ the meron evolution that we advocate would occur at much smaller gyromagnetic ratio (or stronger interaction strength). Further merons of higher meron number ($n=2$ or 3), “giant merons,” are highly unlikely in larger droplets, $N > 5$, as described in Ref. 16. This will likely cause that implied $N/2$ periodicity would be slightly modified, as entering merons would accommodate also on orbitals away, off the center just in the case of vortex excitations in the completely polarized case.²⁰

To illustrate the bulk single meron configuration that the construction in Eq. (2) for $n=1$ represents we plotted in Fig. 5 its spin density $\mathbf{S}(z)$, and charge density $\rho(z)$, as functions of the 2D coordinate $z=|z|\exp(i\varphi)$ in the case of $N=20$. The analytic expressions (which are plotted) for spin density $\mathbf{S}(z)$ are

$$S_z(z) = (N - |z|^2)f_N(|z|), \quad (7)$$

$$S_x(z) = 2\sqrt{N}|z|\cos(\varphi)f_N(|z|), \quad (8)$$

$$S_y(z) = 2\sqrt{N}|z|\sin(\varphi)f_N(|z|), \quad (9)$$

and for charge density $\rho(z)$ is

$$\rho(z) = (N + |z|^2)f_N(|z|), \quad (10)$$

where

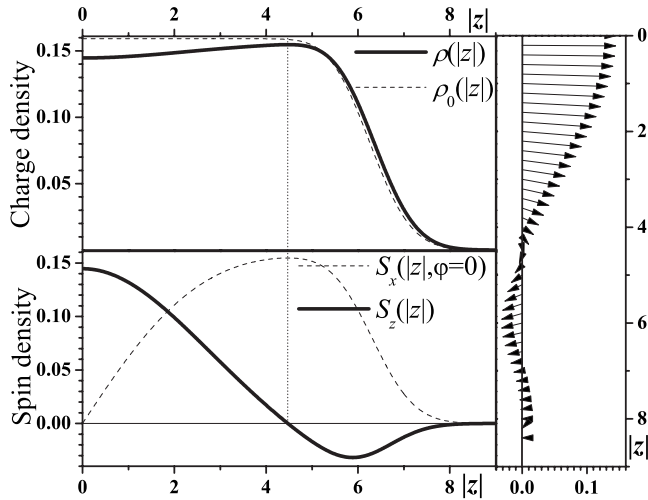


FIG. 5. Plotted are for $N=20$, in the upper panel, charge density $\rho(|z|)$ with respect to the density in the ground state, $\rho_0(|z|)$, in the lower panel, $S_z(|z|)$ component of the spin density along $S_x(|z|, \varphi=0) = \sqrt{S_x^2(|z|) + S_y^2(|z|)}$, and in the side panel, spin-density vector $\mathbf{S}(|z|)$ as functions of radius $|z|$ for the meron construction, Eq. (2) with $n=1$. A small dip in the charge density for $|z| < \sqrt{N}$ describes the deficit of the charge due to the presence of a meron. The amount of the missing charge is $0.486e$, close to $e/2$ as expected for a meron.

$$f_N(|z|) = \sum_{m=0}^{N-1} \frac{|z|^{2m} e^{-|z|^2/2}}{2\pi 2^{m+1} m! \left(m + 1 + \frac{N}{2}\right)}. \quad (11)$$

Therefore we have $\mathbf{S}^2(z) = \rho^2(z)$. From Fig. 5 and these expressions we can conclude that for $|z| \leq \sqrt{N}$ we have a description of a single meron that is created in the bulk of the system. Close to the boundary $\mathbf{S}(z)$ vector lies in the 2D plane and rotates for 2π as expected for a meron.

Now, we must pose a question which quantum mechanical states—eigenstates of M and S_z , correspond to the “mean-field” or “classical” constructions expressed by Eq. (2). We will take that each meron classical construction corresponds to the quantum-mechanical state that we find by expanding the spinor part of Eq. (2) with eigenvalue of M corresponding to the expectation value in Eq. (3). On the other hand, the states that were proposed for spin (global not only edge) reconstructions in Ref. 22 are of the following form $(\Sigma_1^\dagger)^{k_0} |C_N\rangle$. $|C_N\rangle$ denotes the filled with N spin \uparrow particles LLL, a Vandermonde determinant, and $\Sigma_1^\dagger = \sum_m \sqrt{m+1} c_{m+1, \downarrow}^\dagger c_{m, \uparrow}$, an exciton operator with c_m^\dagger and c_m , the electron creation and annihilation operators, and m denoting single-particle angular momentum. $k_0 = N/2$, if N is even, and after a little inspection we can find out that the state described by the formula coincides with our quantum-mechanical eigenstate analog of the construction in Eq. (2) with n equal to 1. As we now show explicitly, in the case of the merons of Eq. (2), these constructions carry very small S_z . The states in Eq. (2) are eigenstates of $M + nS_z - M_0$ with eigenvalues $nN/2$.¹⁷ Therefore $\langle S_z \rangle$ in these states is $\langle S_z \rangle = -(n-1)/2$ and $n \geq 1$ for merons.

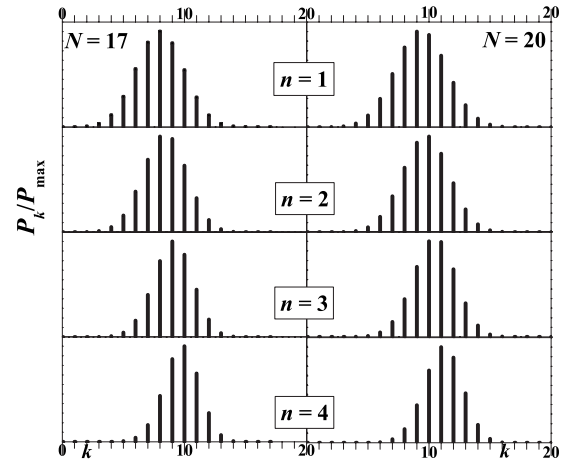


FIG. 6. Participation ratios P_k/P_{\max} of the eigenstates of the angular momentum with eigenvalues $M = N(N-1)/2 + nk$ as functions of $k = 1, \dots, N$ for the meron construction defined by Eq. (2).

To find out whether even in small droplets the mean-field ansatz has a distribution of participating eigenstates of M (and S_z) very much peaked around the quantum-mechanical states with ΔM given in Eq. (3), we calculated these distributions (Fig. 6) in the cases of a droplet with $N=17$ and $N=20$. Although our trial functions are not eigenstates of the angular momentum, the calculated participation ratios,

$$\frac{P_k}{P_{\max}} = \left(\frac{2}{N}\right)^{kn} \times \sum_{\langle i_0, \dots, i_{N-1} \rangle} (0 + i_0 n)! \cdots (N-1 + i_{N-1} n)!, \quad (12)$$

where $i_f = 0, 1$ and $\sum_{f=0}^{N-1} i_f = k$, are indeed well peaked around expectation values,

$$\Delta M(N, n) = \frac{\sum_{k=0}^N nk P_k}{\sum_{k=0}^N P_k}. \quad (13)$$

III. DISCUSSION AND CONCLUSIONS

The meron physics we described above should be, in principle, detectable in lateral quantum dots, in which interaction effects are strong, in their not yet explored regime beyond the MDD state,²³ as well just below the MDD state where depolarized ($S=0$) states were already discovered.⁴ Besides the study in Ref. 16 of small systems, there are studies in Refs. 10, 24, and 25 without the LLL approximation that find depolarized states that we can identify as meron ground states. They appear at angular momenta, multiplets of $N/2$, for N even.

Here we addressed the question of the existence of the meron ground states in larger quantum Hall droplets. Our conclusion is, as long as the Zeeman term is small, the meron ground states are viable solutions of these droplets for N smaller than ~ 100 . Also we expect the appearance of merons in any small enough system of particles with the lowest Landau-level quantization and a degenerate, additional degree of freedom. That may happen in graphene structures in the presence of magnetic field (with valley de-

gree of freedom) or rapidly rotating quantum gases (with spin degree of freedom).

A previous study, Ref. 26, of few-electron quantum dots, without the Zeeman term, was based on restricted (conditional) wave function (RWF) method.¹¹ As the method underlines explicit fixing of the spin projection of each electron, the vortices observed are analogous to those of polarized systems. A more detailed and recent study in Ref. 27 is based on the same method and discusses the problem of two distinguishable species of bosons or fermions which rapidly rotate. As usual in these circumstances the LLL approximation is applied and the fermion system is (up to the difference caused by the distinguishability) the same as in the case of the quantum Hall droplet discussed in this paper. The first vortices that enter the MDD come at the increase in angular momentum of $N/2$. Due to being just vortices of one kind of fermions, a density of fermions of another kind at their core was detected. Because of this phenomenon these vortices are called coreless vortices. For a larger droplet ($N=20$) it was demonstrated using density functional theory and the RWF method that a coreless vortex enters the droplet (at an angular momentum slightly higher than that of MDD). Based on these observations, i.e., that coreless vortices as merons show an increase in polarization at their core (center), and our studies we can conclude that merons are the solutions of the quantum Hall droplet in the fully spin rotationally invariant case, i.e., in an indistinguishable picture, and correspond to these coreless vortices in the distinguishable picture.

ACKNOWLEDGMENT

This work was supported by Grants No. 141035, No. 141017, and No. 141014 of the Serbian Ministry of Science.

APPENDIX

First we consider a fixed spin configuration—component of the total wave function whose expectation value of the interaction energy we want to calculate

$$\Psi(z_1, \dots, z_N). \quad (\text{A1})$$

Ψ in general does not have any overall definite symmetry property (i.e., it is not antisymmetric or symmetric in general). We first have to perform the calculation for each component Ψ separately and then add contributions. We do the calculation by performing the projection to angular momentum, $l=1$, component of wave function Ψ for each pair of particles z_i and z_j . The component can be extracted by expanding Ψ in powers of (z_i+z_j) and (z_i-z_j) , i.e.,

$$\begin{aligned} \Psi = & \sum_{m,n=0} (z_i - z_j)^m (z_i + z_j)^n \\ & \times C_{m,n}(z_1, \dots, z_{i-1}, z_{i+1}, \dots, z_{j-1}, z_{j+1}, \dots, z_N), \end{aligned} \quad (\text{A2})$$

and taking only $m=1$ contribution—wave function in the expansion. Because we take $V_{l=1}=1$, the normalized, integrated over all coordinates square of the projection would be the contribution to the interaction energy from the given spin configuration Ψ and fixed pair of particles.

¹L. P. Kouwenhoven, D. G. Austing, and S. Tarucha, *Rep. Prog. Phys.* **64**, 701 (2001); M. A. Kastner, *Ann. Phys. (N.Y.)* **9**, 885 (2000); L. Jacak, P. Hawrylak, and A. Wójs, *Quantum Dots* (Springer-Verlag, Berlin, 1998).
²P. A. Maksym and T. Chakraborty, *Phys. Rev. Lett.* **65**, 108 (1990); A. H. MacDonald, S. R. Eric Yang, and M. D. Johnson, *Aust. J. Phys.* **46**, 345 (1993); S. M. Reimann and M. Manninen, *Rev. Mod. Phys.* **74**, 1283 (2002).
³P. L. McEuen, E. B. Foxman, U. Meirav, M. A. Kastner, Yigal Meir, Ned S. Wingreen, and S. J. Wind, *Phys. Rev. Lett.* **66**, 1926 (1991); O. Klein, C. de C. Chamon, D. Tang, D. M. Abusch-Magder, U. Meirav, X.-G. Wen, M. A. Kastner, and S. J. Wind, *ibid.* **74**, 785 (1995).
⁴P. Hawrylak, C. Gould, A. Sachrajda, Y. Feng, and Z. Wasilewski, *Phys. Rev. B* **59**, 2801 (1999).
⁵A. Wójs and P. Hawrylak, *Phys. Rev. B* **56**, 13227 (1997).
⁶M. Korkusiński, P. Hawrylak, M. Ciorga, M. Pioro-Ladrière, and A. S. Sachrajda, *Phys. Rev. Lett.* **93**, 206806 (2004).
⁷H. Imamura, H. Aoki, and P. A. Maksym, *Phys. Rev. B* **57**, R4257 (1998); H. Imamura, P. A. Maksym, and H. Aoki, *Physica B (Amsterdam)* **249-251**, 214 (1998).
⁸S. L. Sondhi, A. Karlhede, S. A. Kivelson, and E. H. Rezayi, *Phys. Rev. B* **47**, 16419 (1993).
⁹K. Moon, H. Mori, S. M. Kun Yang, Girvin, A. H. MacDonald, L. Zheng, D. Yoshioka, and Shou-Cheng Zhang, *Phys. Rev. B*

51, 5138 (1995).

¹⁰S. Siljamaki, A. Harju, R. M. Nieminen, V. A. Sverdlov, and P. Hyvönen, *Phys. Rev. B* **65**, 121306(R) (2002).
¹¹H. Saarikoski, A. Harju, M. J. Puska, and R. M. Nieminen, *Phys. Rev. Lett.* **93**, 116802 (2004).
¹²M. B. Tavernier, E. Anisimovas, and F. M. Peeters, *Phys. Rev. B* **70**, 155321 (2004).
¹³M. Toreblad, M. Borgh, M. Koskinen, M. Manninen, and S. M. Reimann, *Phys. Rev. Lett.* **93**, 090407 (2004).
¹⁴M. Manninen, S. M. Reimann, M. Koskinen, Y. Yu, and M. Toreblad, *Phys. Rev. Lett.* **94**, 106405 (2005).
¹⁵A design for a small average g factor, $|g| \approx 0$, was put forward in G. Salis, Y. Kato, K. Ensslin, D. C. Driscoll, A. C. Gossard, and D. D. Awschalom, *Nature (London)* **414**, 619 (2001).
¹⁶A. Petković and M. V. Milovanović, *Phys. Rev. Lett.* **98**, 066808 (2007).
¹⁷For the justification of this special choice see below. This wave function was introduced in M. V. Milovanović, *Phys. Rev. B* **67**, 205321 (2003).
¹⁸F. D. M. Haldane, in *The Quantum Hall Effect*, 2nd ed., edited by R. E. Prange and S. M. Girvin (Springer-Verlag, New York, 1990).
¹⁹A. H. MacDonald, H. A. Fertig, and Luis Brey, *Phys. Rev. Lett.* **76**, 2153 (1996).
²⁰H. Saarikoski and A. Harju, *Phys. Rev. Lett.* **94**, 246803 (2005).

- ²¹T. H. Oosterkamp, J. W. Janssen, L. P. Kouwenhoven, D. G. Austing, T. Honda, and S. Tarucha, *Phys. Rev. Lett.* **82**, 2931 (1999).
- ²²J. H. Oaknin, L. Martin-Moreno, and C. Tejedor, *Phys. Rev. B* **54**, 16850 (1996).
- ²³A study of $N=5$ electrons in a vertical quantum dot showed partially polarized states beyond the MDD, Y. Nishi, P. A. Maksym, D. G. Austing, T. Hatano, L. P. Kouwenhoven, H. Aoki, and S. Tarucha, *Phys. Rev. B* **74**, 033306 (2006).
- ²⁴M. B. Tavernier, E. Anisimovas, F. M. Peeters, B. Szafran, J. Adamowski, and S. Bednarek, *Phys. Rev. B* **68**, 205305 (2003).
- ²⁵M. B. Tavernier, E. Anisimovas, and F. M. Peeters, *Phys. Rev. B* **74**, 125305 (2006).
- ²⁶N. Yang, J.-L. Zhu, Z. Dai, and Y. Wang, arXiv:cond-mat/0701766 (unpublished).
- ²⁷H. Saarikoski, A. Harju, J. Christensson, S. Bargi, M. Manninen, and S. M. Reimann, arXiv:0812.3366 (unpublished).